Results in Physics 17 (2020) 103083

Contents lists available at ScienceDirect

Results in Physics

journal homepage: www.elsevier.com/locate/rinp

Quantum correlations and coherence in a driven two-qubit system under non-Markovian dissipative effect

K. Berrada[a,b], Bahaaudin Raffah[c], H. Eleuch[d,e]

[a] Department of Physics, College of Science, Imam Mohammad Ibn Saud Islamic University (IMSIU), Riyadh, Saudi Arabia
[b] The Abdus Salam International Centre for Theoretical Physics, Strada Costiera 11, Miramare-Trieste, Italy
[c] Department of Physics, Faculty of Sciences, King Abdulaziz University, Jeddah 21589, Saudi Arabia
[d] Institute for Quantum Science and Engineering, Texas University, College Station, TX 77843, USA
[e] Department of Applied Sciences and Mathematics, College of Arts and Sciences, Abu Dhabi University, Abu Dhabi, United Arab Emirates

ABSTRACT

By considering an exactly solvable model for a driven two non-interacting qubits, each coupled to a bosonic environment with zero temperature, under the non-Markovian dissipative process, we study the variation of coherence and correlations in terms of different physical parameters. We show the influence of the external classical driving field as well as the initial quantum states. Moreover, we highlight the relationship between the coherence, single-qubit population, and correlations according to the physical parameters of the whole system. We reveal that the preservation and enhancement of coherence and correlations may occur by adjusting the strength of the classical driving field, initial states, and non-Markovian effects.

Introduction

Coherence plays a essential role for quantum information in particular for metrology [1–12], it might also be more considerable than entanglement to process the achievement of quantum algorithms [13,14]. Recent investigations have shown that coherence and quantum entanglement present a crucial role in biological systems [15,16]. Correlation is becoming one of most attractive research subjects in quantum physics [17–20]. Most of efforts in quantum information processing are focused on studying, measuring and quantifying the correlations. In other words the research is oriented toward analyzing how to distinguish the quantum correlation (QC) from the classical ones [17,19,21–26]. Several phenomena in various quantum processing tasks are widely depending on entanglement (a specific type of QC). Several studies have explored the way to split system states into separable and entangled states [27,28]. Other Kinds of QC [29–34] present an estimated power to quantum processing and some of them have been observed experimentally[35–37]. QCs have been investigated [23–25], such as quantum discord (QD) [23,24] which has recently attracted a considerable attention. The QD has been used as a powerful tool for some tasks in quantum communication and computation [38,39,41,40]. In Open quantum system [42–45], decoherence and fluctuations and irreversible dissipative dynamics are caused to the interaction between the quantum system and its surroundings. Recently, the dynamics of entanglement and QD in open systems has been discussed [46–51]. It is shown that for Markovian systems, QD is more robust than entanglement. Entanglement sudden death [46,47] can be observed with a non-vanishing QD [48–52].

The research on the effects of the classical driving field is received increasing attention due to the main changes in the different tasks of quantum optics and information. The study of a driven two-state system in the context of non-Markovian dynamics has been introduced [53], where the authors have explored the dissipative dynamics of the driven two-state system for two kinds of reservoirs and they have showed that it is greatly affected by the spectral properties. Li et al. [54] have examined the precision of the parameter estimation of a single driven qubit interacted with a vacuum. They have shown that the precision could be improved and preserved complectly for a great deal of time in the case of non-Markovian regime with the support of classical driving. Recently, Zhang et al. [55] have used an external classical driving field to speed up the evolution of a qubit in a zero-temperature reservoir considering Markovian and non-Marovovian dynamics. In the same context, it is shown that the quantum evolution can be accelerated by a classical-driven system coupled to a photonic crystal waveguide in the existence of a mirror [56]. More recently, it is proven for a qubit system in a photonic crystal waveguide, the entanglement trapping is obtained by adjusting the strength of the classical field and the memory time [57].

Due to the above mentioned importance of coherence and correlations for different quantum technology tasks, it is important to comprehend how these principal resources are linked to each other. More recently, several works have explored the relation between the coherence and different correlations as defined by entanglement as well as QD [58–62]. In this paper, we address this question, and investigate effects that may lead to effective way to protect and enhance the coherence and entanglement. We examine the coherence and correlations for a driven two-qubit system locally immersed in non-Markovian environment at a zero-temperature. We examine if and to what extent

https://doi.org/10.1016/j.rinp.2020.103083
Received 8 February 2020; Accepted 26 March 2020
Available online 06 April 2020

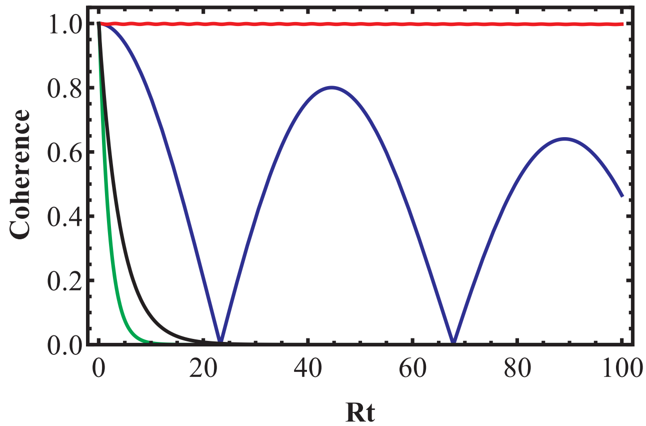

(a)

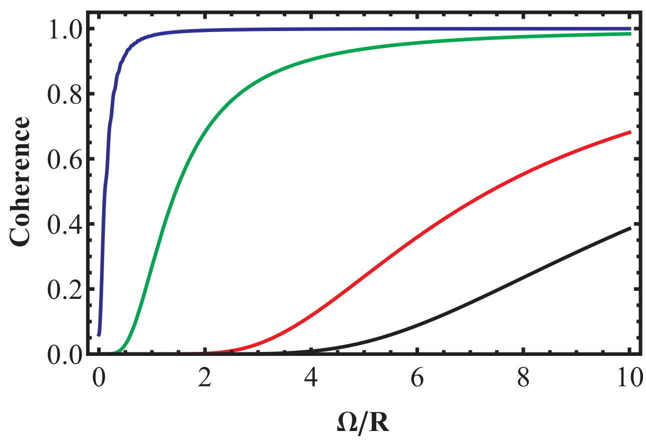

(b)

Fig. 1. Quantum coherence in terms of the dimensionless time Rt and driving strengths Ω/R. Panel (a) shows the coherence as a function of the dimensionless time Rt for the initial qubit state $|\Phi\rangle = 1/\sqrt{2}(|+\rangle + |-\rangle)$ in different driving strengths Ω/R of the external classical field. The blue and red lines exhibit the strong-coupling regime ($\lambda = 0.01R$) for $\Omega/R = 0$ and $\Omega/R = 1$, respectively. The green and black lines exhibit the weak-coupling regime ($\lambda = 10R$) for $\Omega/R = 0$ and $\Omega/R = 5$, respectively. Panel (b) shows the asymptotic behaviors of the coherence as a function of the dimensionless quantity Ω/R with $Rt = 50$ for both strong-coupling and weak-coupling regimes when the initial qubit state is $|\Phi\rangle = 1/\sqrt{2}(|+\rangle + |-\rangle)$. The blue and green lines exhibit the strong-coupling regime for $\lambda = 0.05R$ and $\lambda = 0.5R$, respectively. The red and black lines exhibit the weak-coupling regime for $\lambda = 2.5R$ and $\lambda = 4R$, respectively. (For interpretation of the references to colour in this figure legend, the reader is referred to the web version of this article.)

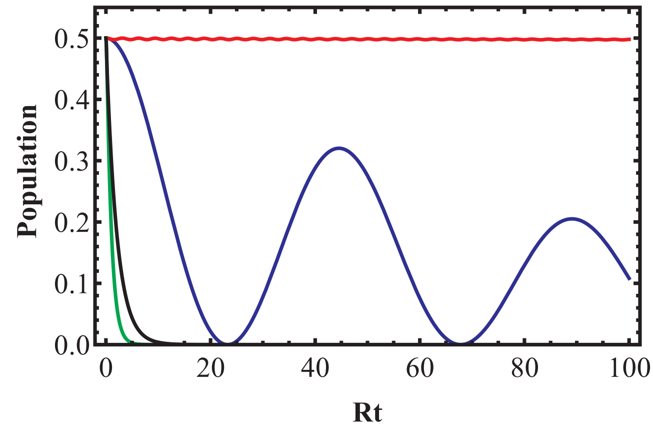

(a)

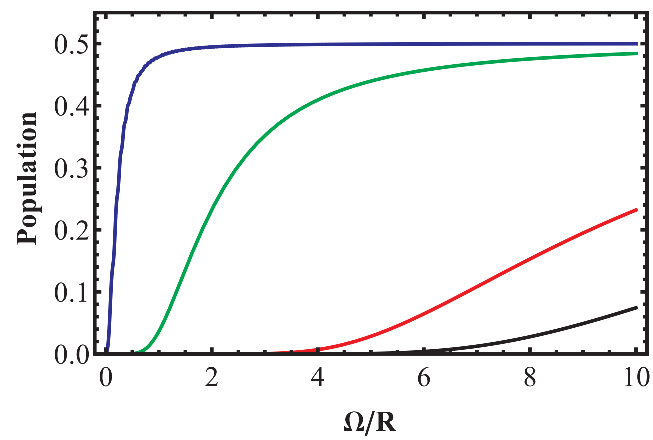

(b)

Fig. 2. Population in terms of the dimensionless time Rt and driving strengths Ω/R. Panel (a) shows the population as a function of the dimensionless time Rt for the initial qubit state $|\Phi\rangle = 1/\sqrt{2}(|+\rangle + |-\rangle)$ in different driving strengths Ω/R of the external classical field. The blue and red lines exhibit the strong-coupling regime ($\lambda = 0.01R$) for $\Omega/R = 0$ and $\Omega/R = 1$, respectively. The green and black lines exhibit the weak-coupling regime ($\lambda = 10R$) for $\Omega/R = 0$ and $\Omega/R = 5$, respectively. Panel (b) shows the asymptotic behaviors of the population as a function of the dimensionless quantity Ω/R with $Rt = 50$ for both strong-coupling and weak-coupling regimes when the initial qubit state is $|\Phi\rangle = 1/\sqrt{2}(|+\rangle + |-\rangle)$. The blue and green lines exhibit the strong-coupling regime for $\lambda = 0.05R$ and $\lambda = 0.5R$, respectively. The red and black lines exhibit the weak-coupling regime for $\lambda = 2.5R$ and $\lambda = 4R$, respectively. (For interpretation of the references to colour in this figure legend, the reader is referred to the web version of this article.)

coherence and correlations initially present may be protected and enhanced for a set of pure and mixed states of qubit pairs. We explicitly show that, for non-Markovian environments with the applied classical field, high values of the amount of coherence and correlations can be achieved. Finally, we highlight the relationship between the coherence, population, and correlations.

This paper is structured as follows. In Section "The physical model and quantities", we describe the two-qubit dynamics driven by classical fields in a non-Markovian reservoir and we review the fundamental concepts of coherence and correlations. In Section "The main results", numerical results are presented. The physical phenomena that can be detected in the existence of the classical driving field with non-Markovian dissipative process are explained. Finally, the conclusion is given in Section "Conclusion".

The physical model and quantities

We consider a qubit system immersed in a zero temperature structured reservoir. The system which consists of a qubit system, of a transition frequency ω_0, that interact with an electromagnetic field. Furthermore, the qubit system is driven by an applied classical field with the frequency ω_F. The Hamiltonian reads [55]

$$H = \frac{\omega_0}{2}\sigma_z + \sum_k \omega_k a_k^\dagger a_k + \Omega(e^{-i\omega_F t}\sigma_+ + e^{i\omega_F t}\sigma_-) + \sum_k g_k(a_k\sigma_+ + a_k^\dagger\sigma_-), \tag{1}$$

where the operators σ_z and $\sigma_\pm$ are described by $\sigma_z = |u\rangle\langle u| - |l\rangle\langle l|$, $\sigma_+ = |u\rangle\langle l|$, and $\sigma_- = \sigma_+^\dagger$ which are defined by the excited level $|u\rangle$ and the ground state $|l\rangle$;a_k ($a_k^\dagger$) is the annihilation (creation) operator for the field with mode k, which is characterized through the frequency ω_k;Ω and g_k describing the coupling constants of

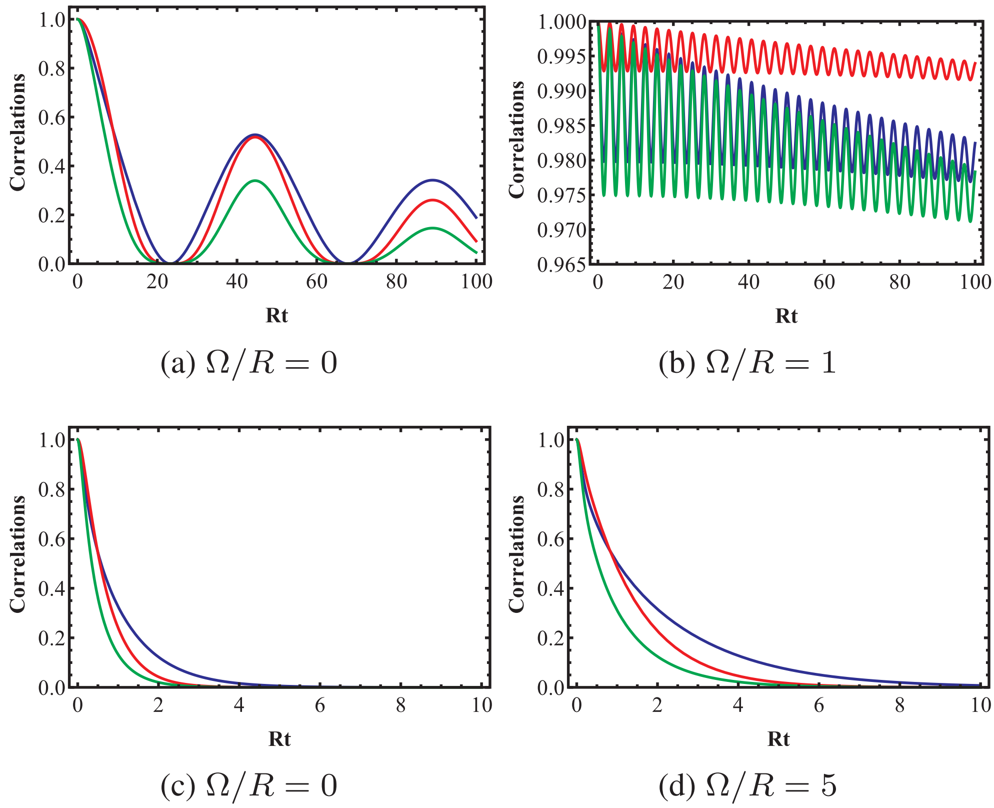

Fig. 3. Quantum and classical correlations as a function of the dimensionless time Rt for the initial Bell state $|\Psi\rangle = 1/\sqrt{2}(|+-\rangle + |-+\rangle)$ in different driving strengths Ω/R of the external classical field. Panels (a) and (b) exhibit the strong-coupling regime ($\lambda = 0.01R$), where panels (c) and (d) exhibit the weak-coupling regime ($\lambda = 10R$). The blue solid line is for the quantum discord, Red solid line is for the entanglement of formation, and green solid line is for the classical correlation. (For interpretation of the references to colour in this figure legend, the reader is referred to the web version of this article.)

the qubits with the classical driving field and with field mode k, respectively. The frequency Ω is assumed to be small compared to the driving frequency and atomic frequencies [63].

In this manuscript, we assume that the transition frequency of the qubit in resonant with the applied field frequency, i.e., $\omega_0 = \omega_F$. In the dressed-state basis $\{|+\rangle = 1/\sqrt{2}(|l\rangle + |u\rangle), |-\rangle = 1/\sqrt{2}(|l\rangle - |u\rangle)\}$, taking into consideration 2-rotating reference frames through two unitary transformations, $U_1 = \exp[-i\omega_F\sigma_z t/2]$ and $U_2 = \exp[-i\omega_0\Sigma_z t/2]$ [55], four terms of no-conservation energy will occur. According to the rotating wave approximation discussed in Ref. [55], the Hamiltonian defined in Eq. (1) will be transformed into an effective Hamiltonian,

$$H_{\text{eff}} = \frac{\omega'}{2}\Sigma_z + \sum_k \omega_k a_k^\dagger a_k + \sum_k g_k'(a_k\Sigma_+ + a_k^\dagger\Sigma_-), \tag{2}$$

where with $\omega' = 2\Omega + \omega_0$ and $g_k' = g_k/2$. Here Σ_z, and $\Sigma_\pm$ are decribed by $\Sigma_z = |+\rangle\langle+| - |-\rangle\langle-|$, $\Sigma_+ = |+\rangle\langle-|$, and $\Sigma_- = \Sigma_+^\dagger$. A noticeable feature of the transformed Hamiltonian is that the elements of the basis have been amended to $\{|+\rangle, |-\rangle\}$, as the qubit system interacts with its surrounding. We shall now analyze the coherence and correlations for a class of environment that considers the decoherence and dissipation of the two-level system. We consider a Lorentzian spectral density as

$$S(\omega) = \frac{1}{2\pi}\frac{\lambda R}{(\omega - \omega_c)^2 + \lambda^2}, \tag{3}$$

where R presents the coupling strength, λ is the spectral width, and ω_c defines the reservoir center frequency.

We suppose that the qubit system is initially defined in a superposition with a vacuum state, and then in the dressed-state base and in the the context of the non-Markovian dynamics the reduced density operator expression can be given as [55]

$$\hat{\rho}_S(t) = \begin{pmatrix} \rho_{++}(0)|\Xi(t)|^2 & \rho_{+-}(0)\Xi(t) \\ \rho_{-+}(0)\Xi^*(t) & \rho_{--}(0) + \rho_{++}(0)(1 - |\Xi(t)|^2) \end{pmatrix}, \tag{4}$$

where

$$\Xi(t) = e^{[\lambda - i(\omega' - \omega_c)]t/2}\left[\cosh\left(\Theta t/2\right) + \frac{\lambda - i(\omega' - \omega_c)}{\Theta}\sinh\left(\Theta t/2\right)\right], \tag{5}$$

and

$$\Theta = \sqrt{\lambda^2 - 2R\lambda - (\omega' - \omega_c)^2 - 2i(\omega' - \omega_v)\lambda}. \tag{6}$$

Generally, there exist two regimes [64]: strong-coupling regime ($\lambda/2 < R$), where the non-Markovian dynamics takes place, and weak-coupling regime ($\lambda/2 > R$), where the comportment of the quantum-system dynamics is Markovian. The non-Markovian effects become relevant when the correlation time of reservoir will be larger than the relaxation time. Note that for ultrastrong coupling regime, the Rabi model will be more convenient to describe the qubits dynamics and the rotating-wave approximation breaks down. In the considered basis, the single-qubit excited-state population is given by

$$P(t) = \rho_{++}(0)|\Xi(t)|^2. \tag{7}$$

The dynamics of the two-level atom is dependent only on the $\Xi(t)$. The function $\Xi(t)$ contains the environmental spectral density information and the coupling constant. In this context, the dynamical behavior of the coherence and correlations depends on the considered initial states and the Hamiltonian model of (2). To get the expression of the correlations under the classical driving field and non-Markovianity effect, we will identify the density matrix elements of the qubits system.

To describe the standard procedure for obtaining the dynamics of the two qubits, we consider a quantum system with noninteracting parts $\widetilde{A}$ and $\widetilde{B}$ each part containing a qubit $S = A, B$ that is locally

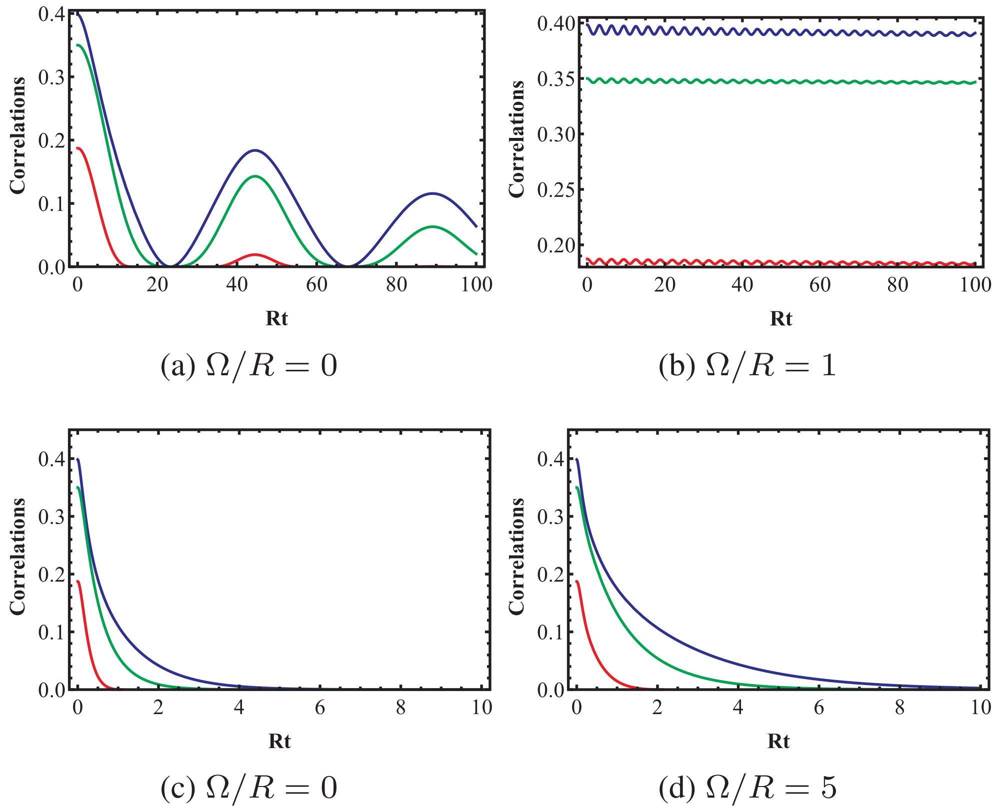

Fig. 4. Quantum and classical correlations as a function of the dimensionless time Rt for the initial entangled mixed state $\rho = 1/3[(1-a)|++\rangle\langle ++| + 2|\Psi\rangle\langle\Psi| + a|--\rangle\langle --|]$ in different driving strengths Ω/R of the external classical field with $a = 1/2$. Panels (a) and (b) exhibit the strong-coupling regime ($\lambda = 0.01R$), where panels (c) and (d) exhibit the weak-coupling regime ($\lambda = 10R$). The blue solid line is for the quantum discord, Red solid line is for the entanglement of formation, and green solid line is for the classical correlation. (For interpretation of the references to colour in this figure legend, the reader is referred to the web version of this article.)

interacted with a reservoir $R_S = R_A, R_B$. For each part, the time evolution of the reduced density operator for one qubit is introduced as [65]

$$\hat{\rho}_S(t) = \mathrm{Tr}_{R_S}\{\hat{U}_{\tilde{S}}(t)\hat{\rho}_S(0) \otimes \hat{\rho}_{R_S}(0)\hat{U}^{\dagger}_{\tilde{S}}(0)\}. \tag{8}$$

By way of the Kraus operators $W_S^{\alpha,\beta}(t)$, the Eq. (8) turns into [66]

$$\hat{\rho}_S(t) = \sum_{\alpha\beta} W_S^{\alpha,\beta}(t)\hat{\rho}_S(0)W_S^{\alpha,\beta^{\dagger}}(t). \tag{9}$$

The composite system $\tilde{T} = \tilde{A} + \tilde{B}$ has the time evolution operator $\hat{U}_{\tilde{T}}(t)$ defined as $\hat{U}_{\tilde{T}}(t) = \hat{U}_{\tilde{A}}(t) \otimes \hat{U}_{\tilde{B}}(t)$. According to the Kraus operators, the two-qubit system is characterized by the reduced density matrix

$$\hat{\rho}_T(t) = \sum_{\alpha\beta}\sum_{\gamma\delta} W_A^{\alpha,\beta}(t)W_B^{\gamma,\delta}(t)\hat{\rho}_T(0)W_A^{\alpha,\beta^{\dagger}}(t)W_B^{\gamma,\delta^{\dagger}}(t). \tag{10}$$

Considering the basis $\{|0\rangle, |1\rangle\}$ for the single qubit and inserting the unity operators $I = |0\rangle\langle 0| + |1\rangle\langle 1|$ between Kraus operators and density states in Eq. (9), the time evolution of each qubit takes the form

$$\rho_A^{ii'}(t) = \sum_{ll'} A_{ll'}^{ii'}(t)\rho_A^{ll'}(0), \quad \rho_B^{jj'}(t) = \sum_{mm'} B_{mm'}^{jj'}(t)\rho_B^{mm'}(0). \tag{11}$$

Executing the same approach for $\hat{\rho}_T(t)$ in the form of Eq. (10), the time evolution of the two qubits is written as

$$\hat{\rho}_T^{ii',jj'}(t) = \sum_{ll',mm'} A_{ll'}^{ii'}(t)B_{mm'}^{jj'}(t)\rho_T^{ll',mm'}(0), \tag{12}$$

Clearly from Eqs. (11) and (12) the time evolution of the two-qubit matrix elements can be deduced from the density matrix of the single qubit.

Let us now build the density operator of the qubits system at subsequent times by knowing the time-evolution of single-qubit state (4), as reported by the standard procedure [65]. Therefore, we can get the explicit expression for the evolution of the two qubits in terms of the function $\Xi(t)$. The two-qubit diagonal elements of the state $\hat{\rho}(t)$ are given in terms of the dressed-state basis $\{|++\rangle, |+-\rangle, |-+\rangle, |--\rangle\}$ as

$$\begin{aligned}
\rho_{11}(t) &= \rho_{11}(0)|\Xi(t)|^4\\
\rho_{22}(t) &= \rho_{11}(0)|\Xi(t)|^2(1-|\Xi(t)|^2) + \rho_{22}(0)|\Xi(t)|^2\\
\rho_{33}(t) &= \rho_{11}(0)|\Xi(t)|^2(1-|\Xi(t)|^2) + \rho_{33}(0)|\Xi(t)|^2\\
\rho_{44}(t) &= 1-(\rho_{11}(t)+\rho_{22}(t)+\rho_{33}(t)),
\end{aligned} \tag{13}$$

and the non-diagonal elements

$$\begin{aligned}
&\rho_{12}(t) = \rho_{12}(0)\Xi(t)|\Xi(t)|^2, \quad \rho_{13}(t) = \rho_{13}(0)\Xi(t)|\Xi(t)|^2\\
&\rho_{14}(t) = \rho_{14}(0)\Xi(t)^2, \quad \rho_{23}(t) = \rho_{23}(0)|\Xi(t)|^2\\
&\rho_{24}(t) = \rho_{13}(0)\Xi(t)(1-|\Xi(t)|^2) + \rho_{24}(0)\Xi(t)\\
&\rho_{34}(t) = \rho_{12}(0)\Xi(t)(1-|\Xi(t)|^2) + \rho_{34}(0)\Xi(t),
\end{aligned} \tag{14}$$

with $\rho_{ij}(t) = \rho^*_{ji}(t)$. According to the relation given in Eqs. (13) and (14), we can examine the time variation correlations for the two-level systems in terms of the physical parameters for any initial state.

Baumgratz et al. [67] proposed simple measures of coherence. In the d-dimensional Hilbert space with fixing a specific basis $\{|i\rangle\}$, the incoherent states take the density operators ot the form $\varrho = \sum_{i=1}^{d} p_i|i\rangle\langle i|$. Thus, the distribution of the off-diagonal elements of ϱ can be used to detect the coherence quantity. A useful measure of coherence should verify ceratin conditions such as monotonicity [67]. l_1 norm quantum coherence meets such conditions is defined by

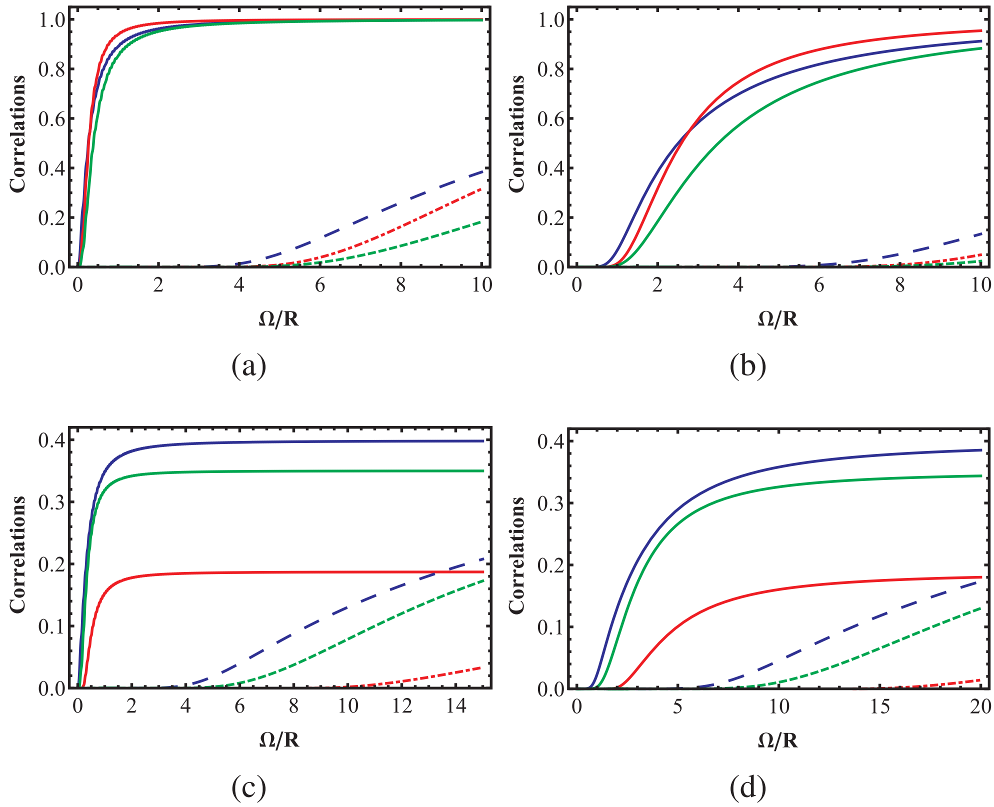

Fig. 5. Asymptotic behaviors of the quantum and classical correlations as a function of the dimensionless quantity Ω/R with $Rt = 50$ for both strong-coupling and weak-coupling regimes. Panels (a) and (b) present the correlations for the initial Bell state $|\Psi\rangle = 1/\sqrt{2}(|+-\rangle + |-+\rangle)$. Panels (c) and (d) present the correlations for the initial entangled mixed state $\rho = 1/3[(1-a)|++\rangle\langle++| + 2|\Psi\rangle\langle\Psi| + a|--\rangle\langle--|]$ with $a = 1/2$. In (a) and (c) the strong-coupling regime is for ($\lambda = 0.05R$) and the weak-coupling regime is for ($\lambda = 2.5R$), where in (b) and (d) the strong-coupling regime is for ($\lambda = 0.5R$) and the weak-coupling regime is for ($\lambda = 4R$). The blue solid (strong-coupling regime) and blue dashed (weak-coupling regime) lines present the quantum discord, the red solid (strong-coupling regime) and red dash-dotted (weak-coupling regime) lines present the entanglement of formation, and the green solid (strong-coupling regime) and green dotted (weak-coupling regime) lines present the classical correlation. (For interpretation of the references to colour in this figure legend, the reader is referred to the web version of this article.)

$$C_{l_1}(\rho) = \sum_{i\neq j} |\rho_{i,j}|. \quad (15)$$

The entanglement of formation (EOF) is a quantifier of entanglement, drawn up about twenty-one years ago [68]. In the case of two-qubit system, Wootters introduced an analytical solution in terms of concurrence [69]. It can be evaluated by

$$E(\rho) = H\left[\frac{1+\sqrt{1-C^2(\rho)}}{2}\right], \quad (16)$$

where H is a function defined by

$$H = -x\log_2 x - (1-x)\log_2(1-x), \quad (17)$$

and

$$C(\rho) = \max\{0, \sqrt{\lambda_1} - \sqrt{\lambda_2} - \sqrt{\lambda_3} - \sqrt{\lambda_4}\}, \quad (18)$$

where λ_i are the eigenvalues listed in decreasing order of $\rho\tilde{\rho}$. $\tilde{\rho}$ denotes the time-reversed density operator

$$\tilde{\rho} = (\sigma_y \otimes \sigma_y)\rho^*(\sigma_y \otimes \sigma_y) \quad (19)$$

where ρ^* is the complex conjugate of the state ρ and σ_y defines the Pauli y operator. We mention that the EOF takes the values $E = 0$ for a separable state and $E = 1$ for a maximally entangled state.

On the other hand, the QD was primarily determined through the mutual information, where the latter is identified as the QC minus the classical correlation (CC) [23], and it is given by the well know formula [24]:

$$\delta_{AB}^{\leftarrow} = \mathscr{I}(\rho_{AB}) - \max_{\{\Pi_k\}} \mathscr{I}\left(\rho_A \middle| \{\Pi_k\}\right) \quad (20)$$

where $\mathscr{I}(\rho_{AB})$ describes the mutual quantum information (MQI), which detects the total correlations and the quantity $\max_{\{\Pi_k\}}\mathscr{I}(\rho_A|\{\Pi_k\})$ is obtained when a measurement is executing over the quantum subsystem B, and it describes the maximal classical mutual information [24,23]. If ρ_A and ρ_B are the reduced density matrix of subsytem A and B, respectively, subsequently the MQI is given as

$$\mathscr{I}(\rho_{AB}) = S(\rho_A) + S(\rho_B) - S(\rho_{AB}) \quad (21)$$

where S. denotes the von Neumann entropy. The CC is defined as:

$$\mathscr{C}_{AB}^{\leftarrow} = \max_{\{\Pi_k\}} \mathscr{I}\left(\rho_A \middle| \{\Pi_k\}\right) = S(\rho_A) - \min_{\{\Pi_k\}} \sum_k p_k S\left(\rho_A \middle| \{\Pi_k\}\right), \quad (22)$$

where, $\rho_A|\{\Pi_k\} = \mathrm{Tr}_B(\Pi_k\rho_{AB}\Pi_k)[\mathrm{Tr}_{AB}(\Pi_k\rho_{AB}\Pi_k)]^{-1}$ defines the reduced operator state of subsystem A after getting the outcome k in subsystem B and Π_k defines the set of positive operator valued measures in the outcome k with the probability $p_k = \mathrm{Tr}_{AB}(\Pi_k\rho_{AB}\Pi_k)$. The QD is definitely given by

$$\delta_{AB}^{\leftarrow} = \mathscr{I}(\rho_{AB}) - \mathscr{C}_{AB}^{\leftarrow}. \quad (23)$$

The indicated definition is a nonsymmetric formulae with regard to the choice of the quantum subsystems and it is constantly positive. The definition of CC in Eq. (22) displays an optimization problem.

Nevertheless, the QD can be determined for generic cases [70,71].

The main results

In order to demonstrate the effect of the classical driving field on the coherence and different kinds of correlations, in Figs. 1–5, we plot the dynamics of the coherence measure, QD, EOF, and CC with respect to different strength of the driving field for Markovian and non-Markovian regimes. In this manuscript, we assume that the transition frequency of the qubit system in resonance with the center mode of the reservoir, i.e., $\omega_0 = \omega_c$ with $R = 1$.

In Fig. 1, (a), the dynamics of coherence for the initial optimal state can be compared with reference to Markovian and non-Markovian environment for various strengths of the classical driving field Ω/R. The blue and red lines are corresponding to the strong-coupling regime for $\Omega/R = 0$ and $\Omega/R = 1$, respectively. The green and black lines are corresponding to the weak-coupling regime for $\Omega/R = 0$ and $\Omega/R = 5$, respectively. It is worth noting that the driving field may partially retard the coherence loss for the case of the Markovian dynamics, but the coherence measure still exponentially decays to zero with the time. Whereas for the non-Markovian dynamics, the dynamical behaviour of coherence is different as in the Markovian one. The coherence displays damped oscillations in the absence of the classical driving field. By reason of the long correlation time of the non-Markovian reservoir, the influx of information backs to the qubit system from reservoir as a result of the memory effect. On the other hand, we observe that the presence of classical driving field in the non-Markovian regime strictly affects the dynamics of the coherence. We observe that the presence of the classical driving field can enhance and preserve the coherence from the non-Markovian environmental effects, where the increasing in the strength of the driving field leads to the increase of the coherence. In Fig. 1(b), we plot the asymptotic behaviors of the coherence in terms of the dimensionless quantity Ω/R with $Rt = 50$ for both strong-coupling and weak-coupling regimes. The blue and green lines exhibit the strong-coupling regime for $\lambda = 0.05R$ and $\lambda = 0.5R$, respectively. The red and black lines exhibit the weak-coupling regime for $\lambda = 2.5R$ and $\lambda = 4R$, respectively. Generally, we observe that the coherence measure increases with the decrease of the λ/R. This can be explained by the fact that more information can be returned to the two-level system for smaller value λ/R accompanied by an enhancement of the non-Markovian effect. Whereas, for smaller non-Markovian effects, the coherence can be enhanced by augmenting the strength of the classical driving field. We also observe that the maximal value of coherence occurs at a some values of driving strength of the classical field Ω_c. When $\Omega_c < \Omega$, the coherence of the two-level system increases monotonically with the enhancement of Ω. In addition, the value of Ω_c is dependent on the parameter λ. Smaller value of λ is, more non-Markovianity effect and it becomes easier to restore the coherence by the driving field. In the case of the weak-coupling regime, only a insignificant part of coherence could be enhanced and protected. These results proved that the preservation and enhancement of coherence is benefited considerably from the combination of strength of the classical field and the memory effect of the environment. In Fig. 2, we show the population variation in terms of the dimensionless quantities Ω/R and Rt, respectively, with respect to the different physical parameters. From the figures, it is clearly shown, that the population exhibits similar behavior as the coherence. This shows that the physical interpretation of the coherence enhancement depends on the relationship between the dynamics of coherence and the population for the two-level system. Whenever the enhancement and preservation of the population is occurring, coherence enhancement and preservation follows.

We now examine the time variation of the quantum and classical correlations for the driven two-qubit system under non-Markovian dissipative effect. In Figs. 3 and 4, we plot the correlations as a function of dimensionless quantities Rt for various values of Ω/R for initial pure and mixed states. The blue line is for the QD, red line is for the EOF, and green line is for the CC. We observe that the dynamics of correlations versus time is influenced by the strength of the classical driving Ω during the quantum evolution. The correlations decay with time almost monotonously for Markovian environments. However, the increase of Ω may retard the correlation loss during the dynamics. The smaller value of Ω is, the correlations decay speeds up always more. The drop phenomenon of the correlations can be understood from the fact that the correlation time is larger than the correlation time of the reservoir and $\Xi(t)$ is a Markovian exponential decay. For the non-Markovian dynamics, the plots show that the correlations oscillate in the absence of classical driving field and exhibit rapid oscillations for non-vanishing Ω. Moreover, the amount and the order of the correlations are significantly affected by the purity of the initial state of the two qubits. Within this regime, $\Xi(t)$ displays oscillations with a quasi-coherent exchange of energy between the qubits and its environments. To get an intuitive comprehension of the influences of the applied field strengths and the non-Markovian features on the asymptotic behaviour of the correlations (classic and quantum), we show in Fig. 5 the correlations in terms of the dimensionless quantity Ω/R for $Rt = 50$. In particular, we observe that the shape of the correlations is similar to the coherence. From this result, we deduce that the enhancement of the correlations can be caused by an appropriate adjusting of the initial state and strength of the classical driving field.

Conclusion

We have examined the dynamics of coherence and correlations in a driven two-qubit system. This system is interactiong with zero-temperature non-Markovian reservoirs. We have analyzed to what extent coherence and correlations initially present may be protected and enhanced for a class of pure and mixed states of non-interacting qubit pairs. Our results indicate that the coherence and correlations can be drastically improved and enhanced by an appropriate adjusting the classical driving field performed on the qubits. We have proven that, for non-Markovian environments with the driving strength of the applied classical field, high values of the amount of coherence and correlations can be achieved. Finally, we highlighted the relationship between the coherence, population, and correlations. An important study will be devoted to the study of the influences of temperature environments on the dynamics of coherence and correlations with a classical driving field. Our present work, from the point of view of phenomenological, might permit the explanation of some experimental observations of the coherence and correlations under the influence of a realistic environment giving further indications for future investigation on this topic.

CRediT authorship contribution statement

K. Berrada: Conceptualization, Methodology, Writing - original draft, Writing - review & editing. **Bahaaudin Raffah:** Validation, Supervision, Project administration. **H. Eleuch:** Validation, Funding acquisition, Investigation.

Declaration of Competing Interest

The authors declare that they have no known competing financial interests or personal relationships that could have appeared to influence the work reported in this paper.

Acknowledgements

This work was supported by the Deanship of Scientific Research (DSR), King Abdulaziz University, Jeddah, under grant No. (D- 266 -130-1441). The authors, therefore, gratefully acknowledge the DSR technical and financial support.

References

[1] Streltsov A, Adesso G, Plenio MB. Rev Mod Phys 2017;89:041003.
[2] Zurek WH. Rev Mod Phys 2003;75:715.
[3] Berrada K. Phys Rev A 2013;88:013817.
[4] Berrada K. Phys Rev A 2013;88:035806.
[5] Berrada K, Eleuch H. Phys Rev D 2019;100:016020.
[6] Berrada K, Eleuch H. Laser Phys Lett 2017;14:095203.
[7] Berrada K. J Opt Soc Am B 2015;32:571.
[8] Berrada K. J Opt Soc Am B 2017;34:1912.
[9] Castelano K, Fanchini FF, Berrada K. Phys Rev B 2016;94:235433.
[10] Berrada K. Laser Phys 2014;24:065201.
[11] Giovannetti V, Lloyd S, Maccone L. Nat Photon 2011;5:222.
[12] Marvian I, Spekkens RW. Phys Rev A 2016;94:052324.
[13] Hillery M. Phys Rev A 2016;93:012111.
[14] Matera JM, Egloff D, Killoran N, Plenio MB. Quantum Sci Technol 2016;1:01LT01.
[15] Huelga S, Plenio M. Contemporary Phys 2013;54:181.
[16] El-Shishtawy RM, Haddon Robert, Al-Heniti Saleh, Raffah Bahaaudin, Abdel-Khalek Sayed, Berrada Kamal, Al-Hadeethi Yas. Energies 2016;9:1063.
[17] Datta A, Gharibian S. Phys Rev A 2009;79:042325.
[18] Berrada K. Open Syst Inf Dyn 2013;20:1350001.
[19] Berrada K, Khalek Abdel, Raymond Ooi CH. Phys Rev A 2012;86:033823.
[20] Sete EA, Svidzinsky AA, Rostovtsev YV, Eleuch H, Jha PK, Suckewer S, Scully MO. IEEE J Selected Topics Quantum Electron 2012;18:541.
[21] Berrada K, Abdel-Khalek S, Eleuch H, et al. Quantum Inform Process 2013;12:69.
[22] Piani M, et al. Phys Rev Lett 2008;100:090502.
[23] Ollivier H, Zurek WH. Phys Rev Lett 2001;88:017901.
[24] Henderson L, Vedral V. J Phys A 2001;34:6899.
[25] Oppenheim J, et al. Phys Rev Lett 2002;89:180402.
[26] Horodecki M, et al. Phys Rev A 2005;71:062307.
[27] Alber G, Beth T, Horodecki M, Horodecki P, Horodecki R, Rotteler M, et al. Quantum Information. Berlin: Springer-Verlag; 2001. Chap. 5.
[28] Horodecki P, Horodecki M, Horodecki K. Rev Mod Phys 2009;81:865.
[29] Mazzola L, Piilo J, Maniscalco S. Phys Rev Lett 2010;104:200401.
[30] Dakić B, Vedral V, Brukner C. Phys Rev Lett 2010;105:190502.
[31] Modi K, Paterek T, Son W, Vedral V, Williamson M. Phys Rev Lett 2010;104:080501.
[32] Datta A, Shaji A, Caves CM. Phys Rev Lett 2008;100:050502.
[33] Niset A, Cerf NJ. Phys Rev A 2006;74:052103.
[34] Sete EA, Eleuch H, Das S. Phys Rev A 2011;84:053817.
[35] Jin-Shi Xu, et al. Nat Commun 2010;1:7.
[36] Lanyon BP, Barbieri M, Almeida MP, White AG. Phys Rev Lett 2008;101:200501.
[37] Datta A, Shaji A, Caves Carlton M. Phys Rev Lett 2008;100:050502.
[38] Cavalcanti D, Aolita L, Boixo S, Modi K, Piani M, Winter1 A. Phys Rev A 2011;83:032324.
[39] Cui J, Fan H. J Phys A: Math Theor 2010;43:045305.
[40] Groisman B, Popescu S, Winter A. Phys Rev A 2005;72:032317.
[41] Lanyon BP, Barbieri M, Almeida MP, White AG. Phys Rev Lett 2008;101:200501.
[42] Campisi M, Talkner P, Hänggi P. Phys Rev Lett 2009;102:210401.
[43] Viola L, Knill E, Lloyd S. Phys Rev Lett 1999;82:2417.
[44] Eleuch H, Rotter I. Phys Rev A 2017;95:022117.
[45] Eleuch H, Rotter I. Phys Rev D 2014;68:74.
[46] Maziero J, Werlang T, Fanchini FF, Céleri LC, Serra RM. Phys Rev A 2010;81:022116.
[47] Almeida MP, et al. Science 2007;316:579.
[48] Werlang T, Souza S, Fanchini FF, Villas Boas C. Phys Rev A 2009;80:024103.
[49] Maziero J, Céleri LC, Serra RM, Vedral V. Phys Rev A 2009;80:044102.
[50] Mazzola L, Piilo J, Maniscalco S. Phys Rev Lett 2010;104:200401.
[51] Pal AK, Bose I. J Phys B: At Mol Opt Phys 2011;44:045101.
[52] Ferraro A, Aolita L, Cavalcanti D, Cucchietti FM, Acin A. Phys Rev A 2010;81:052318.
[53] Haikka P, Maniscalco S. Phys Rev A 2010;81:052103.
[54] Li Yan-Ling, Xiao Xing, Yao Yao. Phys. Rev A 2015;91:052105.
[55] Zhang Ying-Jie, Han Wei, Xia Yun-Jie, Cao Jun-Peng, Fan Heng. Phys Rev A 2015;91:032112.
[56] Wang J, Wu YN, Xie ZY. Sci Rep 2018;8:16870.
[57] Wang Jing, Yunan Wu, Guo Na, Xing Zhen-Yu, Qin Yue, Wang Pei. Opt Commun 2018;420:183.
[58] Macieszczak Katarzyna, Levi Emanuele, Macrì Tommaso, Lesanovsky Igor, Garrahan Juan P. Phys Rev A 2019;99:052354.
[59] Yoshitaka Inui, Yoshihisa Yamamoto, arXiv:1905.12348 (2019).
[60] Fan Zeyang, Peng Yi, Zhang Yu-Ran, Liu Shang, Liang-Zhu Mu, Fan Heng. Sci Rep 2019;9:268.
[61] Yuan Xiao, Zhou Hongyi, Mile Gu, Ma Xiongfeng. Phys Rev A 2018;97:012331.
[62] Wang Xiao-Li, Yue Qiu-Ling, Chao-Hua Yu, Gao Fei, Qin Su-Juan. Sci Rep 2017;7:12122.
[63] Li Yan-Ling, Xiao Xing, Yao Yao. Phys Rev A 2015;91:052105.
[64] Dalton BJ, Barnett SM, Garraway BM. Phys Rev A 2001;64:053813.
[65] Bellomo B, Lo Franco R, Compagno G. Phys Rev Lett 2007;99:160502.
[66] Kraus K. States, effect, and operations: fundamental notions in quantum theory. Berlin: Springer-Verlag; 1983.
[67] Baumgratz T, Cramer M, Plenio MB. Phys Rev Lett 2014;113:140401.
[68] Bennett CH, DiVincenzo DP, Smn JA, Wootters WK. Phys Rev A 1996;54:3824.
[69] Wootters WK. Phys Rev Lett 1998;80:2245.
[70] Luo S. Phys Rev A 2008;77:042303.
[71] Ali M, Rau ARP, Alber G. Phys Rev A 2010;81:042105.